

# CATALYTIC DEGRADATION OF NORFLOXACIN BY PERSULFATE WITH CERIUM NANOCOMPOSITE TEA BIOCHAR

WANG, Y. D.<sup>1\*</sup> – HUANG, C. X.<sup>2</sup>

<sup>1</sup>*Beijing Zhonghuan Carbon Neutral Technology Co., Ltd, Beijing 100080, China*

<sup>2</sup>*Dornsife College of Letters Arts and Sciences, University of Southern California, Los Angeles  
90017, USA*

*(e-mail: chuang85@usc.edu; ORCID: 0009-0009-3872-1974)*

*\*Corresponding author*

*e-mail: carbonwyd2001@163.com; ORCID: 0009-0000-1778-9093*

(Received 4<sup>th</sup> Feb 2025; accepted 22<sup>nd</sup> Apr 2025)

**Abstract.** To create cost-effective, eco-friendly, and efficient catalysts, this research effectively synthesized CeO<sub>2</sub>/BC catalysts from waste tea biochar (BC) by modifying biochar with cerium chloride, and utilized them to initiate persulfate (PDS) for the breakdown of Norfloxacin (NOR). Results demonstrated that the CeO<sub>2</sub> alteration produced a porous, irregular shape on the surface of tea biochar and significantly enhanced the crystallinity of the material's surface. Secondly, FTIR spectroscopy confirmed the effective doping of Cerium onto the biochar surface, substantially increasing the concentration of surface functional groups. Thirdly, the NOR degradation trials indicated that the ideal catalyst dosage was 400 mg/L, PDS dosage was 160 mg/L, pH was 7.1, and the initial NOR concentration was 10 mg/L, resulting in a NOR removal rate of 95.19%. The functions of ·OH and ·SO<sub>4</sub>· in the reduction of NOR were demonstrated by the quenching test. Both species functioned equivalently as catalysts in the CeO<sub>2</sub>/BC system activated by PDS for NOR degradation. Finally, the NOR elimination after 8 cycles diminished to 81.75%, whereas the CeO<sub>2</sub>/BC combination continued to exhibit substantial catalytic activity. The catalyst exhibits attributes of sustainable synthesis and high efficiency in organic matter degradation, indicating potential to scalable use.

**Keywords:** *free radicals, FTIR, reusability, impregnation-pyrolysis method, cerium*

## Introduction

Water resources are vital natural assets essential for human survival; however, the overexploitation of marine ecosystems and the rise in anthropogenic activities have led to significant contamination of the natural aquatic environment (Argaluz et al., 2021). Pharmaceuticals and their metabolites are significant water pollutants of concern due to their environmental persistence and detrimental consequences. Research indicates that antibiotic pollutants from pharmaceutical industries, human waste, and hospital effluents can range from one nanogram per liter to several hundred milligrams per liter (Tahrani et al., 2016; Balarak et al., 2020). The presence of antibiotics in natural aquatic environments has the potential to produce harmful effects on aquatic organisms, disrupting the equilibrium of the aquatic ecosystem. Consequently, examining the remediation of antibiotic contaminants in aquatic environments is of practical importance.

Over the past few decades, researchers have employed physical, chemical, and biological strategies to eliminate antibiotic pollutants from water, including adsorption (Mangla et al., 2022), biodegradation (Oberoi et al., 2019), and improved oxidation processes (Elmolla et al., 2010). The advanced oxidation process utilizing

Peroxydisulfuric acid (PDS) activation has garnered significant interest due to its simplicity and efficacy in the comprehensive treatment of antibiotic wastewater, attributed to its substantial free radical generation, straightforward operation, and high treatment efficiency (Honarmandrad et al., 2023; Tian et al., 2022; Pirsaeheb et al., 2020). The activation techniques of PDS primarily include of thermal (Norzaee et al., 2018), UV (Pirsaeheb et al., 2019), ultrasonic (Gao et al., 2022), graphene (Forouzesh et al., 2019), alkali (Kang et al., 2016) and transition metal (Li et al., 2023). While these activation methods can successfully activate PDS, they invariably present issues such as secondary contamination, elevated energy usage, and environmental repercussions. Consequently, there is an immediate necessity to establish a robust, eco-friendly, and effective activation mechanism for PDS. Biochar (BC) is an economically viable, sustainable, and aromatic solid material characterized by a rich structural composition. Researchers indicate that BC, possessing abundant functional groups, a high surface area, and a customizable porous structure, exhibits a notable ability for PDS activation (Kemmu et al., 2018). Unmodified biochar has inadequate catalytic activity owing to its instability and insufficient functional group coverage; thus, enhancing the catalytic performance of biochar is essential (Zhang et al., 2021; Shi et al., 2022). Meanwhile, biochar-based degradation catalysts have poor stability and risk of heavy metal release in real wastewater/simulated wastewater. Therefore, it is necessary to develop biochar-based antibiotic degradation catalysts with excellent stability and reusability. Recent studies have been based on the strategy of loading transition metals on the surface of biochar to enhance the active sites of the material to improve the radical generation efficiency of biochar catalysts. However, the easy leaching of transition metals makes these materials less stable (Han et al., 2022). Ce is a characteristic rare earth metal with ample availability, economical cost, and non-toxicity. Han et al. (2022) have indicated that cerium oxides proficiently store and release oxygen via the redox cycling of  $\text{Ce}^{3+}$  and  $\text{Ce}^{4+}$ , a characteristic that can result in the creation of unstable oxygen vacancies within the bulk phase of cerium oxides, significantly enhancing the electronic conversion of multi-component catalysts. Hence, the incorporation of Ce onto charcoal can mitigate issues related to metal oxide agglomeration and ion leaching, while simultaneously enhancing the catalyst's efficacy.

This study involved the preparation of  $\text{CeO}_2$  modified tea biochar ( $\text{CeO}_2/\text{BC}$ ) using impregnation pyrolysis, which was utilized for the activation of peroxydisulfate (PDS) to breakdown norfloxacin. The primary research is as follows:

- (1) XRD, SEM, and FTIR were initially used to analyze the microstructure, crystal shape, and surface functional groups of  $\text{CeO}_2/\text{BC}$ .
- (2) The degradation efficiencies of norfloxacin were examined according on catalyst dosage, PDS dose, pH value, and varying starting concentrations.
- (3) The primary reactive oxygen species were identified using free radical burst studies, and the mechanism of NOR degradation in the  $\text{CeO}_2/\text{BC}/\text{PDS}$  system has been investigated with the goal of establishing an experimental basis for the enhanced removal of antibiotic wastewater.

## Materials and methods

### Reagents

The reagents utilized in the experiments, including perchloric acid, sodium persulfate, sodium nitrate, cerium sulfate, methanol, isopropanol, tert-butanol, sodium

hydroxide, hydrochloric acid, sodium carbonate, cerium dioxide, sodium bicarbonate, potassium iodide, etc., were of superior purity and procured from Shanghai Hu Reagent Co. A standard sample of norfloxacin (100 µg/mL) was acquired from Beijing BioBW Biotechnology Co. The waste tea residue is taken from Anxi, Fujian Province, and the tea type is oolong tea.

### Material preparation

The preparation of tea biochar (BC) involved the collection of discarded tea dregs prior to the experiment, which were thereafter stored in the laboratory. The tea dregs were repeatedly cleaned with deionized water and meticulously chopped into little pieces using scissors. Thereafter, the pulverized tea dregs underwent pyrolysis in a tube furnace (YHGS-120612, Shanghai Yuzhe Technology Co., Ltd.) under a nitrogen atmosphere at 600°C for 60 min to produce tea biochar (BC), which was subsequently ground and crushed using a grinder (IN~T2L, Shandong Laiyin Optoelectronics Technology Co., Ltd.) and filtered via a 100-mesh-screen.

The synthesis of CeO<sub>2</sub> modified tea biochar (CeO<sub>2</sub>/BC) was conducted utilizing the impregnation-pyrolysis technique. The preparation procedure is illustrated in the *Figure 1*.

Initially, 0.5 g of tea biochar and a specified volume of 0.1 M cerium chloride solution were introduced into a beaker, establishing a mass ratio of tea powder to cerium chloride of 1:0.5. Subsequently, 5 mL of ultrapure water was incorporated, and the mixture was subjected to stirring on a stirrer (L-220, Lai Heng Science and Technology Co., Ltd.) for a duration of 12 h. Upon completion of the stirring phase, a 1 M NaOH solution was incrementally added to the mixture to elevate the pH above 11, followed by a 3-h incubation period. Subsequent to the resting period, the mixture was subjected to centrifugation using a TGL-16M centrifuge. The solution was allowed to stand for 3 h. Following this, it was centrifuged at 8000 r/min for 3 min, and the supernatant was subsequently washed three times with ethanol and ultrapure water. The centrifuged product was desiccated in a constant temperature oven at 100°C overnight and subsequently sieved through a 100-mesh screen. Subsequent to drying, the biochar precursor was positioned in a tube furnace and subjected to a temperature of 600°C at a heating rate of 5°C/min for a duration of 2 h. CeO<sub>2</sub>-modified tea biochar was acquired following the cooling process.

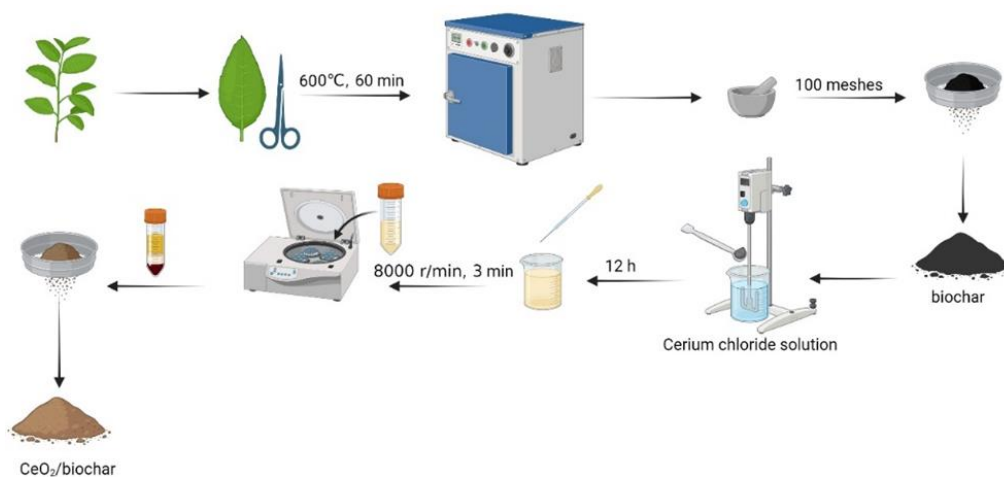


**Figure 1.** Preparation procedure of CeO<sub>2</sub>-modified tea biochar

### ***Structural and performance characterization***

This study analyzed the concentration of norfloxacin in degradation products using a liquid chromatograph (model LC3600, Anhui Wan Yi Technology Co., Ltd.). The pH of the solution was determined using a pH meter (model HZP-T502, Huazhi Electronic Science and Technology Co., Ltd.). The crystalline phase of the samples was examined using an XRD diffractometer (model TK-XRD-201, Beijing Taikun Industrial Equipment Co., Ltd.). Scanning was conducted under the following conditions: 40 kV, 30 mA,  $\lambda = 0.154$  nm, and  $0.02^\circ/\text{s}$  within the  $2\theta$  range of 15 to  $80^\circ$ . FT-IR spectroscopy was performed using a spectrophotometer (Model MPAII, Bruker, Germany) with the KBr disc method. A field-emission scanning electron microscope (Model SEM4000Pro, National Instruments Quantum Technologies Co.) was used to create SEM pictures of the materials.

### ***Adsorption degradation assessment***

CeO<sub>2</sub>/BC activated PDS was used to treat a 10 mg/L NOR solution at a concentration of 50 mL under the conditions of 100-400 mg/L catalyst dosing, 40-160 mg/L PDS dosing, pH range of 2.5-10.9, initial NOR concentration of 10-30 mg/L, and reaction time of 0-60 min. Experiments were performed. All experiments were conducted within a thermostatic oscillator chamber and shielded from light exposure. At the sampling cycle, 2.5 mL of reaction solution was pipetted using a pipette gun, filtered through a 0.22  $\mu\text{m}$  microporous filter and then 0.5 mL of 0.1 M methanol was used to terminate the reaction, after which the NOR concentration was analyzed using liquid chromatography. At the final stage of the experiment, the biochar material was retrieved through centrifugation with a centrifuge, afterwards re-centrifuged using ethanol and ultrapure water, and then dried in a thermostatic oven at 80°C for 10 h. The material was subsequently dried in a thermostatic oven for 10 h.

## **Results and discussion**

### ***Material structure analysis***

The surface morphology of the samples was investigated using field emission scanning electron microscopy, and the findings are shown in *Figure 2a-c*. *Figure 2* illustrates that the CeO<sub>2</sub> sample possesses a bulk structure with a rough surface, whereas the biochar BC exhibits a smooth and non-porous morphology. Furthermore, the SEM image of CeO<sub>2</sub>/BC reveals a porous and irregular spherical structure on the material's surface, indicating the uniform deposition of CeO<sub>2</sub> nanoparticles on the BC surface.

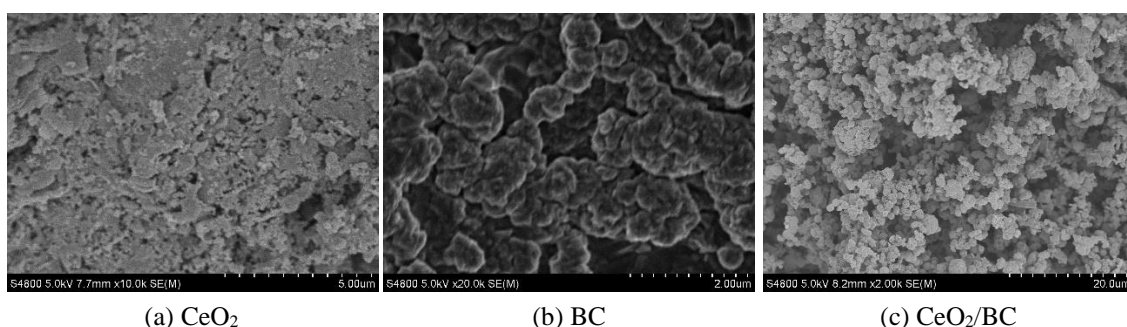


***Figure 2. Microscopic morphology of CeO<sub>2</sub>, BC and CeO<sub>2</sub>/BC***

Figure 3 displays the experimental results of the subsequent XRD diffractometer analysis of the crystal orientation of the different samples. As presented in Figure 3, the peaks of the pure  $\text{CeO}_2$  sample correspond to a face-centered cubic fluorite structure with crystal planes (100), (200), (220), (311), (222), (400), and (420). The commercial  $\text{CeO}_2$  exhibits pronounced and sharp diffraction peaks in the XRD pattern analysis, signifying a high degree of crystallinity in these crystal planes of the material. The diffraction peaks (100), (200), and (311) associated with  $\text{CeO}_2$  were observed in the XRD diffractograms of the  $\text{CeO}_2/\text{BC}$  material, demonstrating the presence of cerium in tea biochar as  $\text{CeO}_2$ .

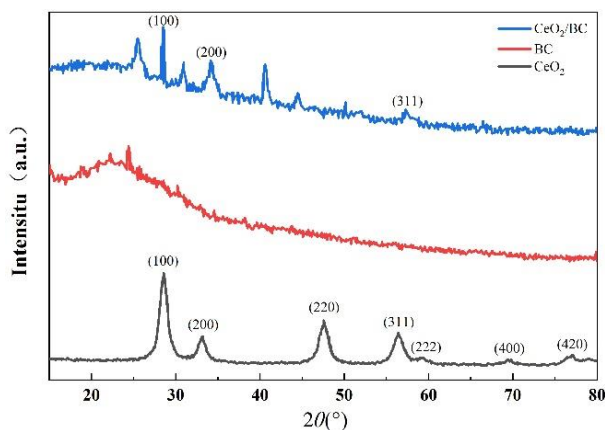


Figure 3. XRD diffractograms of  $\text{CeO}_2$ , BC and  $\text{CeO}_2/\text{BC}$

The surface functional groups in the biochar BC derived from tea dregs and the cerium oxide-modified biochar  $\text{CeO}_2/\text{BC}$  were analyzed using FTIR spectroscopy. From Figure 4, the analyzed results reveal absorption peaks attributed to the stretching of the C = C bond and O-H stretching vibration at  $1395\text{ cm}^{-1}$  and  $3383\text{ cm}^{-1}$ , respectively. The peak at  $1620\text{ cm}^{-1}$  is associated with the C = C/C = O vibration, likely due to the increased adsorption of surface oxygen by the oxygen vacancies in  $\text{CeO}_2$ , facilitating the generation of reactive oxygen species and the breakdown of contaminants. Confirmation of the successful doping of cerium onto the biochar surface is provided by the absorption peak at  $564\text{ cm}^{-1}$ , which is attributed to the stretching vibration of the Ce-O bond.

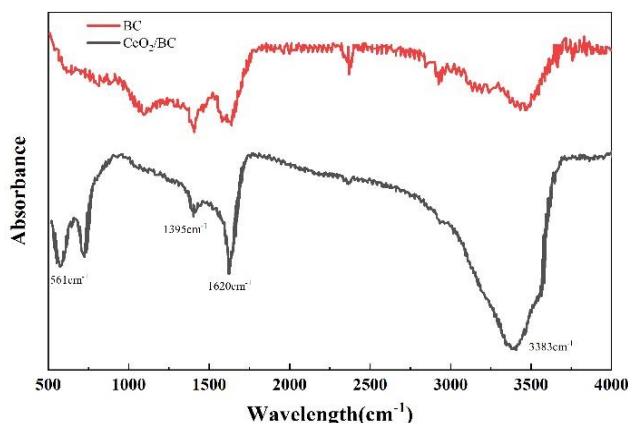
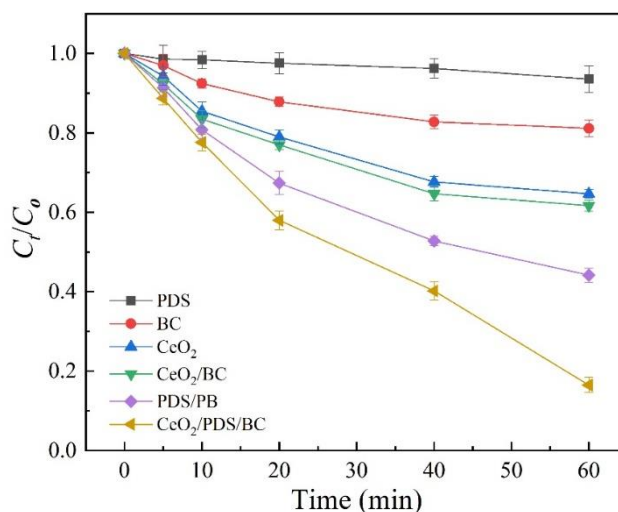


Figure 4. FTIR spectra of BC and  $\text{CeO}_2/\text{BC}$

### Degradation properties of different materials

To analyze the function of each component in the NOR degradation system utilizing  $\text{CeO}_2/\text{BC}$  activated PDS, experiments were conducted to assess the degradation efficiency of various materials for NOR after 60 min of reaction under the conditions of 200 mg/L catalyst dosage, 120 mg/L PDS dosage, pH 7.1, and an initial NOR concentration of 10 mg/L. From *Figure 5*, the pairs of PDS, BC,  $\text{CeO}_2$  and  $\text{CeO}_2/\text{BC}$  exhibited percentages of 6.47%, 18.86%, 35.35% and 61.6%, respectively, after 60 min of reaction. The elimination of NOR by PDS was minimal, suggesting that its direct oxidation of NOR was limited. The removal of NOR induced by the adsorption of PDS/BC and  $\text{CeO}_2/\text{BC}/\text{PDS}$  was 55.82% and 83.51%, respectively, indicating that the distinct functional groups in BC and  $\text{CeO}_2$  can adsorb a portion of the NOR through  $\pi$ - $\pi$  interactions, hydrogen bonding, and electron-pair donor or acceptor reactions. Consequently, the enhanced NOR removal by PDS/BC and  $\text{CeO}_2/\text{BC}/\text{PDS}$  may be due to the active sites enriched in BC and  $\text{CeO}_2/\text{BC}$  being less effective in oxidizing the NOR compared to their oxidation of the NOR. The enhanced active sites in BC promote the breakdown of PDS, yielding  $\cdot\text{OH}$  and  $\cdot\text{SO}_4^-$  (Wang et al., 2023; Guan et al., 2019).



**Figure 5.** Analysis of degradation efficiency of different materials

### Optimization of NOR degradation conditions

#### Catalyst dosage

$\text{CeO}_2/\text{BC}$  activates PDS to generate free radicals such as  $\cdot\text{OH}$  and  $\cdot\text{SO}_4^-$  and provides free radicals with active sites for binding NOR molecules (Han et al., 2022). Therefore, increasing the catalyst dosing is expected to have a significant effect on the degradation efficiency of NOR. The reaction conditions such as PDS dosing of 120 mg/L, pH 7.1 and initial NOR concentration of 10 mg/L were controlled to be constant in the experiments to investigate the effect of different  $\text{CeO}_2/\text{BC}$  dosages (100, 200, 300 and 400 mg/L) on the removal rate of NOR. After 60 min of reaction, the NOR removal rate of the system could reach 58.86%, 69.82%, 81.59%, and 94.50% when the  $\text{CeO}_2/\text{BC}$  dosage was 100, 200, 300, and 400 mg/L, as highlighted in *Figure 6*. Huang et al. (2020) reported the similar results that, in the system of catalyzing PDS, the high concentration of catalysts helps to promote the rate of the decomposition of PDS to

produce radicals such as  $\cdot\text{OH}$  and  $\cdot\text{SO}_4^-$ . Accordingly, the optimum  $\text{CeO}_2/\text{BC}$  catalyst dosage in this study was 400 mg/L.

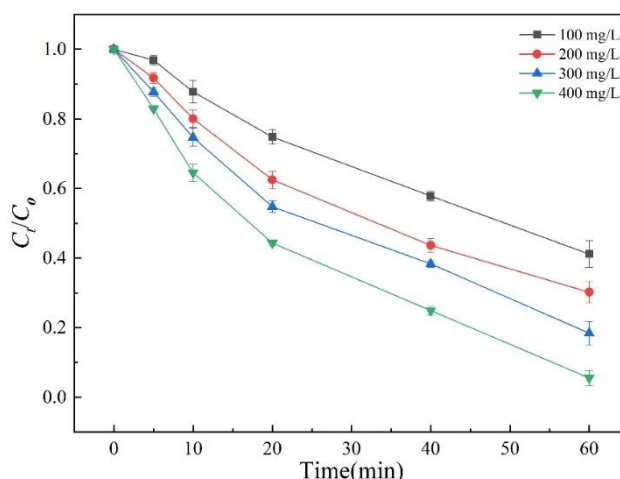


**Figure 6.** Effect of catalyst dosage on NOR removal rate

#### PDS dosing rate

Although the starting concentrations of pollutants and catalysts remain constant, changes in PDS concentration have a substantial impact on the target pollutants' efficiency of degradation because PDS is a precursor to free radicals (Huang et al., 2020). In this section, the catalyst dosage of 200 mg/L, pH 7.1, and the initial NOR concentration of 10 mg/L were controlled unchanged, and the effects of different PDS dosages (40, 80, 120, and 160 mg/L) on the NOR removal were investigated, and the results of the experiment are shown in Figure 7. From Figure 7, the removal rate of NOR increased rapidly with the increase of PDS dosage. The results showed that the removal rate of NOR could reach 55.72%, 72.78%, 82.12% and 95.19% after 60 min reaction time when the PDS dosage was 20, 40, 80 and 160 mg/L, respectively, which might be related to the generation rate of free radicals such as  $\cdot\text{OH}$  and  $\cdot\text{SO}_4^-$  at high oxidant concentration. Therefore, the optimum PDS dosage in this study was 160 mg/L.

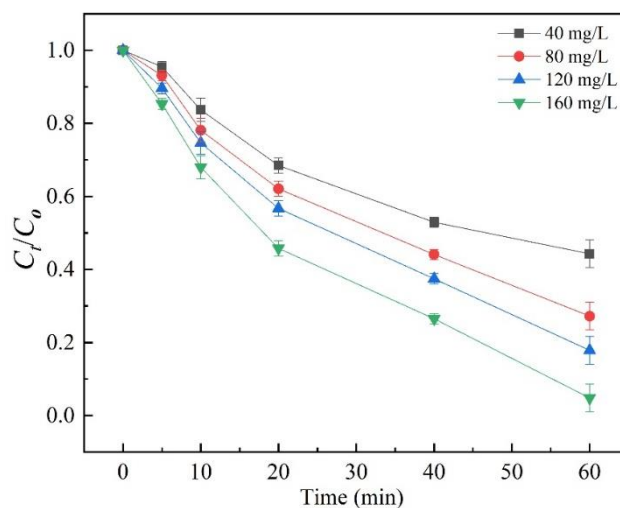


**Figure 7.** Effect of PDS dosage on NOR removal rate



### Acid-base properties

Research indicates that variations in pH influence chemical processes and redox potentials. The generation of active radicals and the surface characteristics of contaminants and nanomaterials (Qian et al., 2020). This section investigated the application scenarios of the  $\text{CeO}_2/\text{BC}$  catalyst by maintaining constant conditions: catalyst injection at 200 mg/L, PDS injection at 120 mg/L, and an initial NOR concentration of 10 mg/L. The effects of pH values of 2.5, 4.8, 7.1, 8.6, and 10.9 on the NOR removal rate were examined, with the experimental results presented in Figure 8. The NOR removal percentages were 48.01%, 60.23%, 84.93%, 76.12%, and 38.47% at pH values of 2.5, 4.8, 7.1, 8.6, and 10.9, respectively. The removal rate of NOR significantly diminished under both highly acidic and highly alkaline conditions. This phenomenon is attributed to the influence of extreme pH levels on the decomposition of PDS and the redox potentials of free radicals, such as  $\cdot\text{OH}$  and  $\cdot\text{SO}_4^-$ , resulting in substantial electrostatic repulsion between NOR and  $\text{CeO}_2/\text{BC}$  at pH values of 2.5 and 10.9, respectively. Furthermore, the negatively charged PDS impedes the electrostatic interaction between NOR and  $\text{CeO}_2/\text{BC}$  at a pH of 10.6, which also obstructs the surface complexation of negatively charged  $\text{CeO}_2/\text{BC}$ , ultimately leading to reduced yields of  $\cdot\text{OH}$  and  $\cdot\text{SO}_4^-$  (Dey et al., 2023). The ideal pH for this study was 7.1.

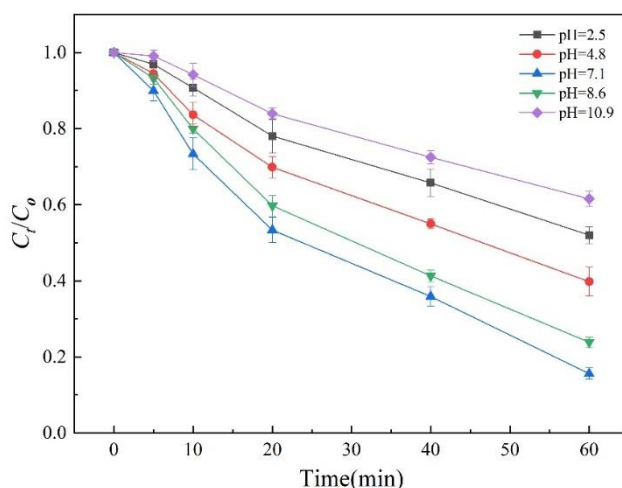


**Figure 8.** Effect of different pH values on NOR removal rate

### Different initial NOR concentrations

The effects on the NOR removal rate were examined while maintaining catalyst dosing at 200 mg/L, PDS dosing at 120 mg/L, and pH at 7.1, with initial NOR concentrations set at 10, 20, and 30 mg/L. Figure 9 displays the results of the experiments. The experimental findings show that NOR exhibits a steady drop as the initial concentration of NOR increases. The removal rate of NOR dropped from 82.59% to 58.86% as its initial concentration rose from 10 mg/L to 30 mg/L. This decline can be attributed to intensified competition for free radicals between residual NOR and intermediates, which may impede the degradation efficiency of NOR. A high concentration of NOR will not only result in rapid consumption of PDS, hindering NOR breakdown, but will also cause excessive NOR aggregation in



CeO<sub>2</sub>/BC, hence restricting PDS diffusion on the material's surface. The ideal initial NOR concentration was 10 mg/L.

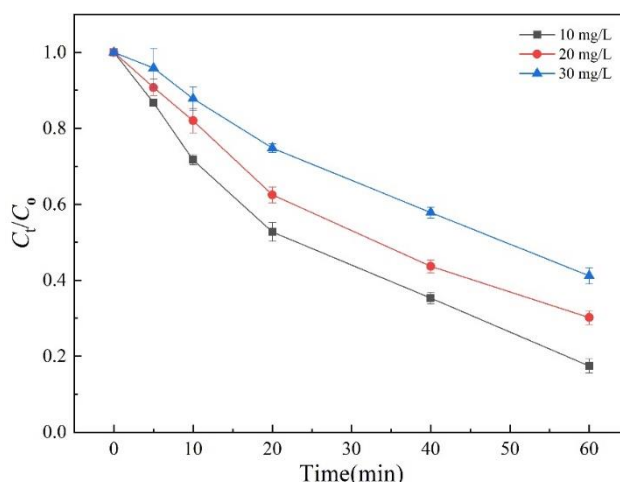


**Figure 9.** Effect of different initial concentration

### Quenching test

Research indicates that isopropanol (IPA) and tert-butyl alcohol (TBA) effectively scavenge hydroxyl radicals ( $\cdot\text{OH}$ ) and sulfate radicals ( $\cdot\text{SO}_4^-$ ) (Dey et al., 2023; Gao et al., 2022). Elevated concentrations of IPA and TBA exhibit superior adsorption capabilities for  $\cdot\text{OH}$  and  $\cdot\text{SO}_4^-$  compared to high concentrations of norfloxacin (NOR). Specifically, IPA reacts with  $\cdot\text{OH}$  at a rate constant of  $k_{\text{OH}/\text{IPA}} = 1.92 \times 10^9 \text{ mol/L}\cdot\text{s}$  and with  $\cdot\text{SO}_4^-$  at  $k_{\text{SO}_4^-/\text{IPA}} = 8.4 \times 10^7 \text{ mol/L}\cdot\text{s}$ , demonstrating its efficacy as a scavenger for these radicals within the reaction system. Scavengers within the reaction system. Conversely, TBA (i.e.,  $k_{\text{OH}/\text{TBA}} = 6.2 \times 10^8 \text{ mol/L}\cdot\text{s}$ ), which exhibits rapid kinetics for  $\cdot\text{OH}$ , was utilized only as a  $\cdot\text{OH}$  scavenger. To analyze the generation of free radicals in the NOR degradation reaction system utilizing the CeO<sub>2</sub>/BC catalyst-activated persulfate, degradation experiments were conducted with 200 mg/L IPA and TBA as quenching agents, 200 mg/L catalyst dosing, 120 mg/L PDS dosing, pH 7.1, and an initial NOR concentration of 10 mg/L. The outcomes of the degradation experiments are illustrated in Figure 10. The experimental results indicate that the NOR removal rate declined to 22.66% and 25.21% with the application of 200 mg/L of IPA and TBA as quenching agents, respectively, demonstrating that CeO<sub>2</sub>/BC activation during PDS breakdown of NOR generated  $\cdot\text{OH}$  and  $\cdot\text{SO}_4^-$  in the system. Both IPA and TBA exhibited nearly identical inhibitory effects, suggesting that  $\cdot\text{OH}$  and  $\cdot\text{SO}_4^-$  are significant contributors to the breakdown of NOR.

### Recycling performance analysis

The recycling ability of the CeO<sub>2</sub>/BC composite was evaluated by recycling experiments and used for subsequent catalytic runs under the same experimental conditions. As can be seen in Figure 11, the NOR removal rate after eight cycles decreased to 81.75%, and the CeO<sub>2</sub>/BC composite still maintained a high catalytic activity, indicating the excellent stability of the material.

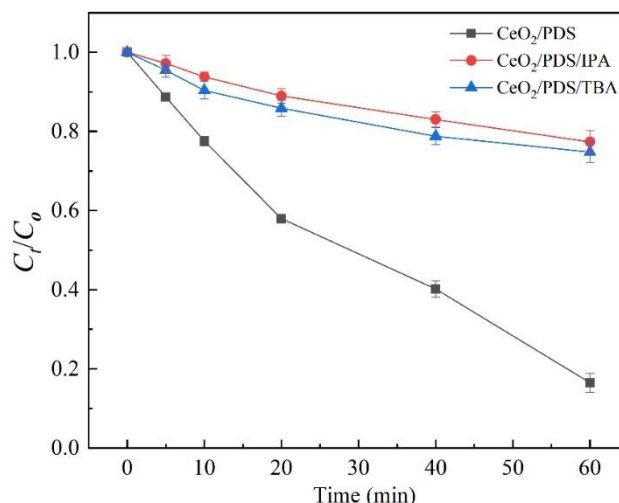


**Figure 10.** Results of quenching test

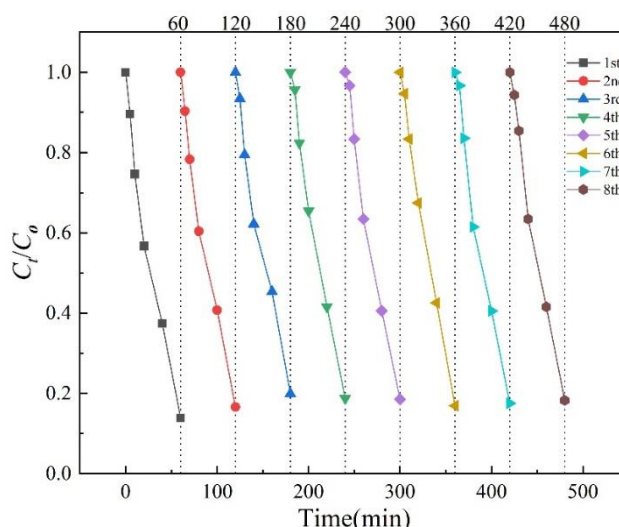


**Figure 11.** Recycling performance analysis

## Conclusions

In this study, CeO<sub>2</sub> modified tea biochar (CeO<sub>2</sub>/BC) was prepared by impregnation pyrolysis and used for the activation of PDS for the degradation of norfloxacin. CeO<sub>2</sub> modification led to a porous and irregular spherical structure on the surface of tea biochar, as well as a substantial increase in the crystallinity of the material surface, as determined by the structural analysis of the material, and secondly, Fourier infrared (FTIR) spectroscopy proved the successful doping of cerium on the surface of the biochar and significantly enriched the concentration of its surface functional groups. At the optimal catalyst dosage of 400 mg/L, PDS dose of 160 mg/L, pH 7.1, and initial NOR concentration of 10 mg/L, the NOR removal rate reached 95.19%. Subsequent quenching test proved the contribution of ·OH and ·SO<sub>4</sub><sup>-</sup> to NOR degradation and that ·OH and ·SO<sub>4</sub><sup>-</sup> freely played the same catalytic roles in the system of CeO<sub>2</sub>/BC activated over PDS degradation of NOR. NOR removal after eight cycles decreased to 81.75% and the CeO<sub>2</sub>/BC composite still maintained a high catalytic activity. The

catalyst has the characteristics of sustainable synthesis and high efficiency of organic matter degradation, which makes it scalable.

This study has some limitations, including the need for further investigation of the catalyst performance under real wastewater conditions, the scalability of the synthesis method, and the potential influence of other environmental factors such as varying pollutant compositions and complex matrices in wastewater. Future studies should aim to address these aspects to enhance the practical application of the catalyst.

## REFERENCES

- [1] Argaluz, J., Domingo-Echaburu, S., Orive, G., Medrano, J., Hernandez, R., Lertxundi, U. (2021): Environmental pollution with psychiatric drugs. – *World Journal of Psychiatry* 11(10): 791. DOI: 10.5498/wjp.v11.i10.791.
- [2] Balarak, D., Khatibi, A. D., Chandrika, K. (2020): Antibiotics removal from aqueous solution and pharmaceutical wastewater by adsorption process: a review. – *International Journal of Pharmaceutical Investigation* 10(2). DOI: 10.5530/ijpi.2020.2.19.
- [3] Dey, A. K., Mishra, S. R., Ahmaruzzaman, M. (2023): Solar light-based advanced oxidation processes for degradation of methylene blue dye using novel Zn-modified CeO<sub>2</sub>@ biochar. – *Environmental Science and Pollution Research* 30(18): 53887-53903. DOI: 10.1007/s11356-023-26183-2.
- [4] Elmolla, E. S., Chaudhuri, M. (2010): Comparison of different advanced oxidation processes for treatment of antibiotic aqueous solution. – *Desalination* 256(1-3): 43-47. DOI: 10.1016/j.desal.2010.02.019.
- [5] Forouzesh, M., Ebadi, A., Aghaeinejad-Meybodi, A. (2019): Degradation of metronidazole antibiotic in aqueous medium using activated carbon as a persulfate activator. – *Separation and Purification Technology* 210: 145-151. DOI: 10.1016/j.seppur.2018.07.066.
- [6] Gao, L., Guo, Y., Zhan, J., Yu, G., Wang, Y. (2022a): Assessment of the validity of the quenching method for evaluating the role of reactive species in pollutant abatement during the persulfate-based process. – *Water Research* 221: 118730. DOI: 10.1016/j.watres.2022.118730.
- [7] Gao, Y., Wang, Q., Ji, G., Li, A. (2022b): Degradation of antibiotic pollutants by persulfate activated with various carbon materials. – *Chemical Engineering Journal* 429: 132387. DOI: 10.1016/j.cej.2021.132387.
- [8] Guan, R., Yuan, X., Wu, Z., Jiang, L., Zhang, J., Li, Y., Mo, D. (2019): Efficient degradation of tetracycline by heterogeneous cobalt oxide/cerium oxide composites mediated with persulfate. – *Separation and Purification Technology* 212: 223-232. DOI: 10.1016/j.seppur.2018.11.019.
- [9] Han, Z., Li, Z., Li, Y., Shang, D., Xie, L., Lv, Y., Hu, W. (2022): Enhanced electron transfer and hydrogen peroxide activation capacity with N, P-codoped carbon encapsulated CeO<sub>2</sub> in heterogeneous electro-Fenton process. – *Chemosphere* 287: 132154. DOI: 10.1016/j.chemosphere.2021.132154.
- [10] Honarmandrad, Z., Sun, X., Wang, Z., Naushad, M., Boczkaj, G. (2023): Activated persulfate and peroxymonosulfate based advanced oxidation processes (AOPs) for antibiotics degradation-A review. – *Water Resources and Industry* 29: 100194. DOI: 10.1016/j.wri.2022.100194.
- [11] Huang, D., Zhang, Q., Zhang, C., Wang, R., Deng, R., Luo, H., Liu, C. (2020): Mn doped magnetic biochar as persulfate activator for the degradation of tetracycline. – *Chemical Engineering Journal* 391: 123532. DOI: 10.1016/j.cej.2019.123532.

- [12] Kang, J., Duan, X., Zhou, L., Sun, H., Tadé, M. O., Wang, S. (2016): Carbocatalytic activation of persulfate for removal of antibiotics in water solutions. – *Chemical Engineering Journal* 288: 399-405. DOI: 10.1016/j.cej.2015.12.040.
- [13] Kemmou, L., Frontistis, Z., Vakros, J., Manariotis, I. D., Mantzavinos, D. (2018): Degradation of antibiotic sulfamethoxazole by biochar-activated persulfate: factors affecting the activation and degradation processes. – *Catalysis Today* 313: 128-133. DOI: 10.1016/j.cattod.2017.12.028.
- [14] Li, N., Ye, J., Dai, H., Shao, P., Liang, L., Kong, L., Duan, X. (2023): A critical review on correlating active sites, oxidative species and degradation routes with persulfate-based antibiotics oxidation. – *Water Research* 119926. DOI: 10.1016/j.watres.2023.119926.
- [15] Mangla, D., Sharma, A., Ikram, S. (2022): Critical review on adsorptive removal of antibiotics: present situation, challenges and future perspective. – *Journal of Hazardous Materials* 425: 127946. DOI: 10.1016/j.jhazmat.2021.127946.
- [16] Norzaee, S., Taghavi, M., Djahed, B., Mostafapour, F. K. (2018): Degradation of Penicillin G by heat activated persulfate in aqueous solution. – *Journal of Environmental Management* 215: 316-323. DOI: 10.1016/j.jenvman.2018.03.038.
- [17] Oberoi, A. S., Jia, Y., Zhang, H., Khanal, S. K., Lu, H. (2019): Insights into the fate and removal of antibiotics in engineered biological treatment systems: a critical review. – *Environmental Science & Technology* 53(13): 7234-7264. DOI: 10.1021/acs.est.9b01131.
- [18] Pirsaeheb, M., Hossaini, H., Janjani, H. (2019): An overview on ultraviolet persulfate based advanced oxidation process for removal of antibiotics from aqueous solutions: a systematic review. – *Water Treat* 165: 382-395. DOI: 10.5004/dwt.2019.24559.
- [19] Pirsaeheb, M., Hossaini, H., Janjani, H. (2020): Reclamation of hospital secondary treatment effluent by sulfate radicals based-advanced oxidation processes (SR-AOPs) for removal of antibiotics. – *Microchemical Journal* 153: 104430. DOI: 10.1016/j.microc.2019.104430.
- [20] Qian, R., Shen, T., Yang, Q., Lin, K. Y. A., Tong, S. (2020): Degradation of isoniazid by graphite loaded CeO<sub>2</sub> activated persulfate. – *Separation and Purification Technology* 250: 117197. DOI: 10.1016/j.seppur.2020.117197.
- [21] Shi, Q., Deng, S., Zheng, Y., Du, Y., Yang, S., Zhang, G., Du, L., Wang, G., Cheng, M. (2022): The application of transition metal-modified biochar in sulfate radical based advanced oxidation processes. – *Environmental Research* 212. DOI: 113340.10.1016/j.envres.2022.113340.
- [22] Tahrani, L., Van Loco, J., Ben Mansour, H., Reyns, T. (2016): Occurrence of antibiotics in pharmaceutical industrial wastewater, wastewater treatment plant and sea waters in Tunisia. – *Journal of Water and Health* 14(2): 208-213. DOI: 10.2166/wh.2015.224.
- [23] Tian, K., Hu, L., Li, L., Zheng, Q., Xin, Y., Zhang, G. (2022): Recent advances in persulfate-based advanced oxidation processes for organic wastewater treatment. – *Chinese Chemical Letters* 33(10): 4461-4477. DOI: 10.1016/j.ccllet.2021.12.042.
- [24] Wang, M., Wang, Y., Li, Y., Wang, C., Kuang, S., Ren, P., Xie, B. (2023): Persulfate oxidation of tetracycline, antibiotic resistant bacteria, and resistance genes activated by Fe doped biochar catalysts: synergy of radical and non-radical processes. – *Chemical Engineering Journal* 464: 142558. DOI: 10.1016/j.cej.2023.142558.
- [25] Zhang, Y., Xu, M., Liang, S., Feng, Z., Zhao, J. (2021): Mechanism of persulfate activation by biochar for the catalytic degradation of antibiotics. Synergistic effects of environmentally persistent free radicals and the defective structure of biochar. – *Science of the Total Environment* 794: 148707. DOI: 10.1016/j.scitotenv.2021.148707.